

THE APPLICATION OF UNKNOWN INPUT ESTIMATORS TO DAMP LOAD OSCILLATIONS OF OVERHEAD CRANES

BÁLINT PATARTICS[✉] AND BÁLINT KISS

Department of Control Engineering and Information Technology, Budapest University of Technology and Economics,
Magyar Tudósok krt. 2, Budapest, 1111, HUNGARY
[✉]E-mail: patarticsbalint@gmail.com

This paper focuses on the development of state estimation methods for mechanical systems with uncertain frictional parameters. The goal of the study is to provide reliable angle estimation for state-feedback-based crane control solutions, designed to reduce load sway. Cranes are underactuated systems, usually unequipped with the sensors necessary to measure the swinging angle, therefore the damping of their oscillatory behaviour is a challenging task. Two estimators are proposed for the calculation of the unmeasured states. One is based on an 'unknown input Kalman filter' (UIKF), the other applies the 'unscented Kalman filter' (UKF) with load prediction. Simulation results are provided to demonstrate the accuracy of the algorithms.

Keywords: overhead crane, state estimation, nonlinear systems, unknown inputs, Kalman filter

Introduction

The sway of the load carried by cranes is an unwanted phenomenon. Friction may decouple load motion from the remaining crane mechanism. This causes difficulty for inexperienced operators, especially when they try to land the cargo. The friction present in the crane mechanism makes the reduction of the swinging particularly demanding. Therefore the goal of the design of crane control systems is often to ensure minimal swinging along a specified trajectory [1–6].

There are numerous algorithms available in the literature for the solution to this problem. The design of such a control system can be addressed using soft computing methods such as fuzzy logic and neural network with genetic algorithm. These solutions require however the measurement of the load position, which is often based on workspace visualization [1]. Hard commuting techniques are also widely applied for sway reduction. An H_2 optimal solution is described in Ref.[2], which also relies on image processing for the measurement of the load coordinates. There are a variety of algorithms taking advantage of the flatness property (or exact linearizability) of overhead cranes [7]. The control systems in Refs.[3] and [4] consider all the states measurable, however an estimator is proposed in Ref.[3] for the computation of the uncertain parameters.

In the case of navy cranes, local asymptotic stability can be achieved without the measurement of the swinging angle, if trajectory planning exploits the flatness property of the system [6]. There is also a tracking control algorithm specifically designed for overhead cranes, that

is capable of effectively reducing the sway despite the friction [5]. For the calculation of the unmeasured states, this controller uses a linear observer. In this paper we propose new methods of state observation for systems that take into account friction, and are applicable to overhead cranes. These estimators can replace the linear observer in Ref.[5] or the need to measure the load coordinates in any other state-feedback-based method to enhance the precision of the control. Our estimation methods are based on the assumption that the effect of the friction on the inputs can be reduced. This is true for most mechanical systems (including overhead cranes), where the actuating signals are usually forces and torques.

In the following section, the modelling of Lagrangian mechanical systems is overviewed, and it is shown how the friction can be handled as an input disturbance. In the next section the state estimation techniques are presented based on the possible approaches of interpreting the friction. The next section describes the results of the application of these methods to the state estimation problem of overhead cranes and presents the simulation results.

Lagrangian-Based Models of Mechanical Systems

The nonlinear dynamics of the controlled system can be obtained using the Euler-Lagrange equations. If the generalized coordinates are $q = (q_1 \ q_2 \ \dots \ q_n)^T$ and the generalized forces are $\tau = (\tau_1 \ \tau_2 \ \dots \ \tau_n)^T$, the Euler-Lagrange equations read

$$\frac{d}{dt} \frac{\partial \mathcal{L}}{\partial \dot{q}_i} - \frac{\partial \mathcal{L}}{\partial q_i} = \tau_i, \quad (1)$$

where \mathcal{L} is the so-called Lagrangian, the difference between the kinetic and potential energy of the system, $\dot{q}_i = \frac{dq_i}{dt}$ and $i = 1, 2, \dots, n$.

Using these equations, under some conditions the controlled system's model can be written in the form

$$H(q)\dot{q} + h(q, \dot{q}) + h_s(s) = \tau, \quad (2)$$

where $H(q)$ is the inertia matrix, $h(q, \dot{q})$ comprises the centrifugal, Coriolis and gravitational terms, and $h_s(s)$ is the frictional term with s being the vector of the frictional forces. In this form $h_s(s)$ can be reorganized to the right-hand-side of the equation. Introducing the disturbance torques as $\tilde{\tau} = \tau - h_s(s)$, Eq.(2) yields

$$H(q)\dot{q} + h(q, \dot{q}) = \tilde{\tau}. \quad (3)$$

The state-space representation of the model is

$$\begin{aligned} \dot{x} &= f(x, u) \\ y &= g(x), \end{aligned} \quad (4)$$

where x is the state, u is the input, y is the output of the system, and f and g are nonlinear functions. This form can be obtained from Eq.(5) assuming that $x^T = (q^T \quad \dot{q}^T)$, and the output is not directly dependent on the torques. The state-space equations read

$$\begin{aligned} \dot{x} &= \begin{pmatrix} \dot{q} \\ -H^{-1}(q)h(q, \dot{q}) \end{pmatrix} + \begin{pmatrix} 0 \\ H^{-1}(q) \end{pmatrix} \tilde{\tau} \\ y &= g(x). \end{aligned} \quad (5)$$

The inputs of mechanical systems are usually forces and torques, consequently they are only dependent on $\tilde{\tau}$. This means, that the effect of the friction can be reduced to the actuated degrees of freedom of the system.

If it is necessary for the design of the control system, the nonlinear dynamics can be approximated by a first order Taylor series expansion around a setpoint (x_0, u_0) . The linear model then becomes

$$\begin{aligned} \delta\dot{x} &= A\delta x + B\delta u \\ \delta y &= C\delta x, \end{aligned} \quad (6)$$

where the quantities prefixed with δ mean the distance from the setpoint, e.g. $\delta x = x - x_0$, and the matrices are Jacobians [8].

State Estimation Methods

Since the friction can be interpreted in our setup as an input disturbance, we consider two ways for its compensation in the state estimation. Either all input variables can be disregarded, or the additive disturbance can be estimated using a load predictor. These ideas form the basis of the two estimator design techniques described as follows.

The computations of the controllers implemented in embedded systems are based on sampled signals. Hence the design of the estimators is done in discrete-time.

Unknown Input Approach

Consider the discrete-time linear stochastic system model

$$\begin{aligned} x[k+1] &= \Phi x[k] + \Gamma_d d[k] + \omega[k] \\ z[k] &= Cx[k] + v[k], \end{aligned} \quad (7)$$

where x is the state, d is the unknown input (disturbance) of the system and z is the measurement of the output $y[k] = Cx[k]$. Φ and Γ_d are obtained from the matrices of Eq.(6) in the form of

$$\Phi = e^{AT_s}, \quad \Gamma_d = \int_0^{T_s} e^{At} B dt, \quad (8)$$

where T_s is the sample time. The measurement and process noise v and ω are assumed to be additive, white, and Gaussian with mean of zero. Notice, that in Eq.(7), all of the system inputs are considered to be disturbances.

The state and the unknown input of such a system can be estimated using an 'unknown input Kalman filter' (UIKF) [9], if the system satisfies the conditions

$$\dim\{d\} \leq \dim\{y\} \quad (9)$$

$$\text{rank}\{C\} = \dim\{y\} \quad (10)$$

$$\text{rank}\{\Gamma_d\} = \dim\{d\} \quad (11)$$

$$\text{rank}\{C\Gamma_d\} = \dim\{d\}. \quad (12)$$

Additive Disturbance Approach

In the case of input disturbances, load prediction is often applied. Let us introduce the discrete-time nonlinear model of a system in the form

$$\begin{aligned} x[k+1] &= \phi(x[k], \tilde{u}[k]) + \omega[k] \\ z[k] &= g(x[k]) + v[k], \end{aligned} \quad (13)$$

where \tilde{u} is the disturbed input of the system, and ϕ and g are nonlinear functions. We will follow the assumption, that the disturbance is additive to the input, thus $\tilde{u}[k] = u[k] + \Lambda d[k]$, where u is the vector of actuating signals, and Λ is a constant matrix.

We also assume a constant disturbance model with process noise ω_d , $d[k+1] = d[k] + \omega_d[k]$, resulting in the model

$$\begin{aligned} \tilde{x}[k+1] &= \tilde{\phi}(\tilde{x}[k], u[k]) + \tilde{\omega}[k] \\ z[k] &= \tilde{g}(\tilde{x}[k]) + v[k]. \end{aligned} \quad (14)$$

In Eq.(14) $\tilde{x}^T = (x^T \quad d^T)$ is the extended state and $\tilde{\omega}^T = (\omega^T \quad \omega_d^T)$ is the extended process noise. The extended nonlinear mappings of the system are given by $\tilde{g}(\tilde{x}[k]) = g(x[k])$ and

$$\tilde{\phi}(\tilde{x}[k], u[k]) = \begin{pmatrix} \phi(x[k], u[k] + \Lambda d[k]) \\ d[k] \end{pmatrix}. \quad (15)$$

In most cases the continuous-time differential equation of the observed system is available, in the form

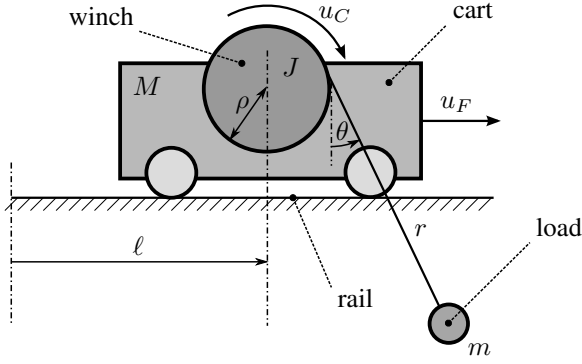


Figure 1: The two-dimensional overhead crane

of Eq.(4). The discrete-time state-transition equation can then be obtained by

$$\phi(x[k], u[k]) = x[k] + \int_{kT_s}^{(k+1)T_s} f(x, u[k]) dt, \quad (16)$$

where the input is piecewise constant and $u[k] = u(kT_s)$. If the integral in Eq.(16) cannot be given in closed form and T_s is sufficiently small, the left rectangle rule approximation

$$\int_{kT_s}^{(k+1)T_s} f(x, u[k]) dt \approx T_s f(x[k], u[k]). \quad (17)$$

can be used. Substituting this into Eq.(15), the expression reads

$$\tilde{\phi}(\tilde{x}[k], u[k]) = \begin{pmatrix} x[k] + T_s f(x[k], u[k] + \Lambda d[k]) \\ d[k] \end{pmatrix}. \quad (18)$$

For the observation of the system described by Eq.(14) and Eq.(18) the 'unscented Kalman filter' (UKF) [10] is applicable. We chose one of the implementation variants of this filter from Ref.[10].

Application of the Methods to Overhead Cranes

System Dynamics

We will now consider the state estimation problem of the two-dimensional overhead crane (Fig.1). Let us denote the horizontal displacement of the cart by ℓ , the length of the rope by r and the angle between the vertical and the rope by θ . The generalized coordinates of the system are chosen to be $q = (\ell \ r \ \theta)^T$, and the state is $x = (\ell \ r \ \theta \ \dot{\ell} \ \dot{r} \ \dot{\theta})^T$. Based on the sensors available, the output is $y = (\ell \ r \ \dot{\ell} \ \dot{r})^T$.

Overhead cranes is a typical example of underactuated systems. It is actuated by two motors, one applying the force u_F on the cart, and another delivering the

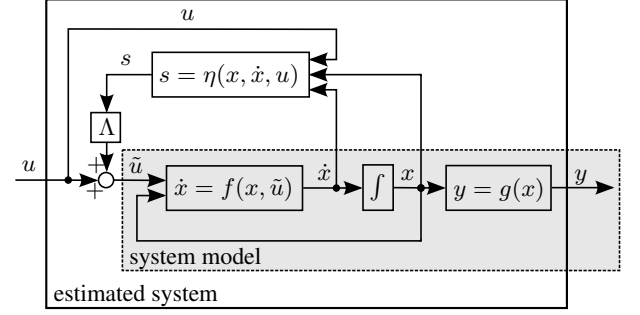


Figure 2: Dynamics of the estimated system

torque u_C to the winch. The system input consists of these, $u = (u_F \ u_C)^T$.

The parameters of the system are the mass of the cart M , the mass of the load m , the moment of inertia of the winch J and the radius of the winch ρ . The acceleration in the gravitational field is denoted by g .

The following assumptions are made of the system.

- The rope connecting the load to the winch is massless and behaves as a rigid rod during the motion.
- The load is a point mass.
- M , m , J and ρ are known.
- In the initial state of the system the unmeasured states are zero: $\theta = 0$ rad and $\dot{\theta} = 0$ rad/s.
- The effect of the aerodynamic resistance is negligible.

The Lagrangian of overhead cranes reads

$$\mathcal{L} = \frac{1}{2} (M + m) \dot{\ell}^2 + \frac{1}{2} \frac{J}{\rho^2} \dot{r}^2 + \frac{1}{2} m (\dot{r}^2 + r^2 \dot{\theta}^2) + m \dot{r} \sin \theta + m \dot{r} \dot{\theta} \cos \theta + m g r \cos \theta. \quad (19)$$

Using Eq.(1), the model can be written in the form of Eq.(2), where the expressions become

$$H(q) = \begin{pmatrix} (M + m \sin^2 \theta) & m \sin \theta & 0 \\ m \sin \theta & \left(\frac{J}{\rho^2} + m\right) & 0 \\ \cos \theta & 0 & r \end{pmatrix}, \quad (20)$$

$$h(q, \dot{q}) = - \begin{pmatrix} m(r \dot{\theta}^2 + g \cos \theta) \sin \theta \\ m r \dot{\theta}^2 + m g \cos \theta \\ -2 \dot{r} \dot{\theta} - g \sin \theta \end{pmatrix}, \quad (21)$$

$$h_s(s) = - \begin{pmatrix} s_F \\ s_C \\ 0 \end{pmatrix}, \quad \tau = \begin{pmatrix} u_F \\ -\frac{u_C}{\rho} \\ 0 \end{pmatrix}, \quad (22)$$

where s_F is the frictional force between the cart and the rail and s_C is the frictional force applied to the winch.

The continuous-time linear model of the crane is computed around the setpoint $x_0 = (0 \ r_0 \ 0 \ 0 \ 0 \ 0)^T$, $u_0 = (0 \ m g \rho)^T$, and $s_F = s_C = 0$ is substituted

Table 1: Numeric values of the parameters

	Value	Unit
M	5	kg
m	0.05	kg
J	$3.802 \cdot 10^{-4}$	kg m ²
ρ	0.02	m
g	9.81	m s ⁻²
T_s	1	ms
r_0	0.47	m
ℓ_D	0.5	m

into Eq.(5). The resulting Jacobians are

$$\begin{aligned}
 A &= \begin{pmatrix} 0 & 0 & 0 & 1 & 0 & 0 \\ 0 & 0 & 0 & 0 & 1 & 0 \\ 0 & 0 & 0 & 0 & 0 & 1 \\ 0 & 0 & \frac{m}{M}g & 0 & 0 & 0 \\ 0 & 0 & 0 & 0 & 0 & 0 \\ 0 & 0 & -\frac{m+M}{Mr_0}g & 0 & 0 & 0 \end{pmatrix}, \\
 B &= \begin{pmatrix} 0 & 0 \\ 0 & 0 \\ 0 & 0 \\ \frac{1}{M} & 0 \\ 0 & -\frac{\rho}{m\rho^2+J} \\ -\frac{1}{Mr_0} & 0 \end{pmatrix}, \\
 C &= \begin{pmatrix} 1 & 0 & 0 & 0 & 0 & 0 \\ 0 & 1 & 0 & 0 & 0 & 0 \\ 0 & 0 & 0 & 1 & 0 & 0 \\ 0 & 0 & 0 & 0 & 1 & 0 \end{pmatrix}.
 \end{aligned} \tag{23}$$

Substituting Eq.(22), the disturbance torque term in Eq.(3) reads

$$\tilde{\tau} = \begin{pmatrix} u_F + s_F \\ -\frac{1}{\rho}(u_C - \rho s_C) \\ 0 \end{pmatrix}. \tag{24}$$

Eq.(24) shows, that the disturbed input of the system can be introduced in the form $\tilde{u} = u + \Lambda s$, where

$$\Lambda = \begin{pmatrix} 1 & 0 \\ 0 & -\rho \end{pmatrix}. \tag{25}$$

The frictional forces usually depend on the actuating signals, state variables, and the derivative of the state as well. The general characteristics of the friction reads as $s = \eta(x, \dot{x}, u)$. The block diagram of the dynamics of the system is illustrated in Fig.2. Only the system model block is used for estimator design, which is Eq.(5) if the effect of the friction is disregarded, $h_s(s) = 0$.

Proposition 1. *The discrete-time linear crane model obtained from the matrices in Eq.(23) and using Eq.(8) satisfies the design conditions of the UIKF in Eq.(9-12).*

Proof. It is clear that $\dim\{y\} = 4$, $\dim\{d\} = 2$ and $\text{rank}\{C\} = 4$, thus Eq.(9) and (10) are satisfied. Us-

ing Eq.(8) and the numerical values in Table 1,

$$\begin{aligned}
 \Gamma_d &= 10^{-2} \begin{pmatrix} 0.0001 & 0 \\ 0 & -0.025 \\ -0.0002 & 0 \\ 0.2 & 0 \\ 0 & -49.975 \\ -0.4255 & 0 \end{pmatrix}, \\
 C\Gamma_d &= 10^{-2} \begin{pmatrix} 0.0001 & 0 \\ 0 & -0.025 \\ 0.2 & 0 \\ 0 & -49.975 \end{pmatrix}.
 \end{aligned} \tag{26}$$

We obtain $\text{rank}\{\Gamma_d\} = 2$ and $\text{rank}\{C\Gamma_d\} = 2$, which are both equal to the number of unknown inputs. This satisfies Eqs.(11) and (12). The continuity argument holds for the rank of the matrices in Eq.(26), therefore there exists a neighbourhood around our parameter set where the design conditions are still satisfied.

Simulation

The estimation results were obtained by simulation of overhead cranes in a closed-loop scenario using a simple discrete-time pole-placement-based linear controller. The simulation also took into account friction. There are various models of the friction phenomenon, ours included Coulomb, Stribeck, viscous friction, and stiction [11]. The numerical values of the parameters used in the simulation are given in Table 1.

Because of friction, but mainly stiction, the position of the crane can not be accurately controlled without integrators in the controller. Consequently we included the integral of the measurable positions in the controller design as proposed on page 309 of Ref. [8].

The outputs to be integrated are $y_I = (\ell \ r)^T$. Integrals of these quantities are approximated by the left rectangle rule as

$$x_I[k+1] = x_I[k] + T_s y_I[k] = x_I[k] + T_s C_I x[k], \tag{27}$$

where C_I is defined so that $y_I[k] = C_I x[k]$. In our case C_I is the first two rows of C in Eq.(23). Using Eq.(27) and Eq.(7) a new system model is introduced in the form

$$\begin{aligned}
 \tilde{x}[k+1] &= \tilde{\Phi}\tilde{x}[k] + \tilde{\Gamma}u[k] \\
 y[k] &= \tilde{C}\tilde{x}[k].
 \end{aligned} \tag{28}$$

where the expanded state is $\tilde{x}^T = (x^T \ x_I^T)$ and the matrices are

$$\begin{aligned}
 \tilde{\Phi} &= \begin{pmatrix} \Phi & 0 \\ T_s C_I & I \end{pmatrix}, \quad \tilde{\Gamma} = \begin{pmatrix} \Gamma_d \\ 0 \end{pmatrix}, \\
 \tilde{C} &= (C \ 0).
 \end{aligned} \tag{29}$$

For the controller design the process and measurement noises are omitted.

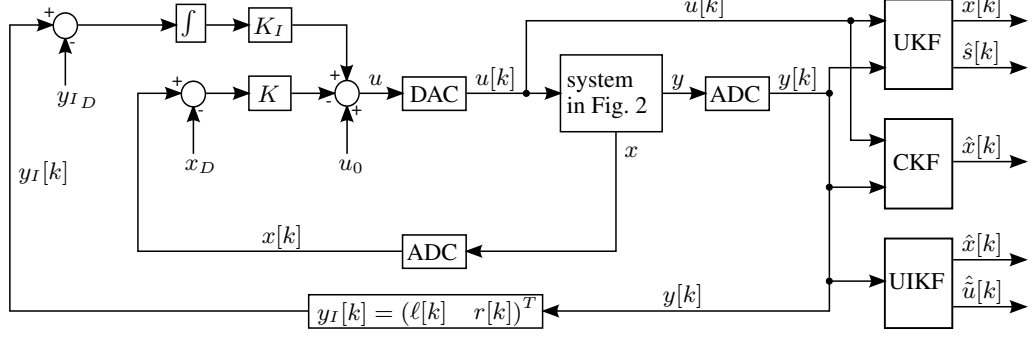


Figure 3: Closed-loop estimation setup used in the simulation

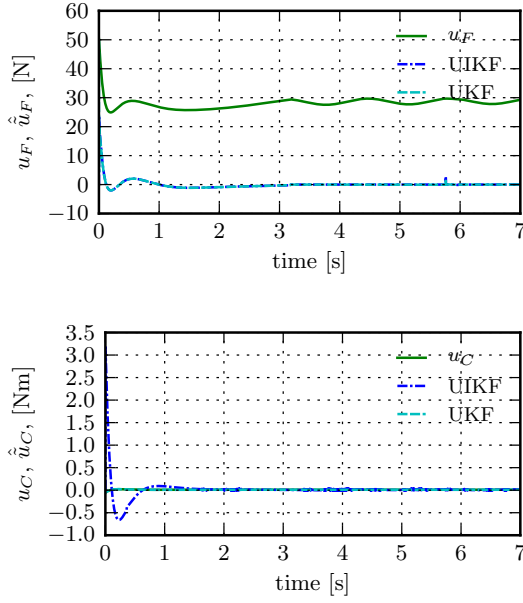


Figure 4: Actuating signals and the estimated inputs of the system

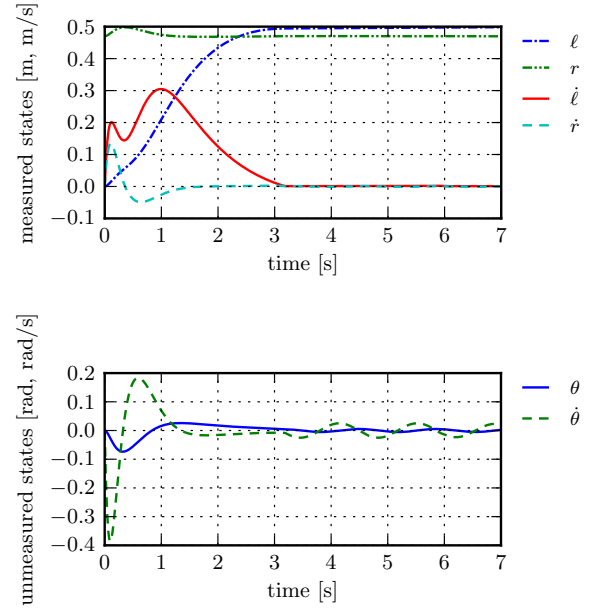


Figure 5: State evolution of the controlled crane using the true states as feedback

We want the state-feedback controller to output $u[k] = -\tilde{K}\tilde{x}[k] = -Kx[k] - K_I x_I[k]$. The gain \tilde{K} can be computed using the eigenvalue placement method implemented in Matlab's `place` algorithm: $\tilde{K} = \text{place}(\tilde{\Phi}, \tilde{\Gamma}, \lambda)$, where λ contains the chosen eigenvalues of the closed-loop system. In continuous time they are $-1 + 0.5j$, $-1 - 0.5j$, -5.1 , -5.2 , -5.3 , -5.4 , -5.5 , and -5.6 . The controller gains are

$$K = \begin{pmatrix} 100.594 & -0.1273 \\ 0.6011 & -1.6765 \\ -185.407 & 0.0458 \\ 81.4011 & -0.0558 \\ 0.0562 & -0.3166 \\ -4.2257 & -0.0195 \end{pmatrix}^T, \quad \text{and} \quad (30)$$

$$K_I = \begin{pmatrix} 46.641 & 1.6026 \\ -0.074 & -2.955 \end{pmatrix}.$$

The closed-loop setup is illustrated in *Fig.3*. Here the integration is done using the left rectangle rule, and the

ADC and DAC blocks are analogue-digital and digital-analogue converters respectively. The DAC uses the zero-order hold method for signal reconstruction. The desired state of the system is $x_D = (\ell_D \ r_0 \ 0 \ 0 \ 0 \ 0)^T$, ℓ_D is the desired position of the cart and $y_{ID} = C_I x_D$.

Since we only want to demonstrate the results of the state estimation, first the real states are fed back to the controller. To compare the accuracy of our methods to a traditional solution, the classical Kalman filter (CKF) [12] is also implemented. As a result, the Kalman filters compute the estimated state of the system $\hat{x}[k]$, and they also provide information about the input.

The UIKF estimates the friction loaded actuating signals directly, while the UKF estimates the frictional forces superposed to the actuating signals. The actuating signals along with the estimates of the real inputs provided by the filters can be seen in *Fig.4*. Here, the estimated input of the UKF is computed as $\hat{u} = u[k] + \Lambda \hat{s}[k]$.

Because of friction, the real inputs are estimated to be

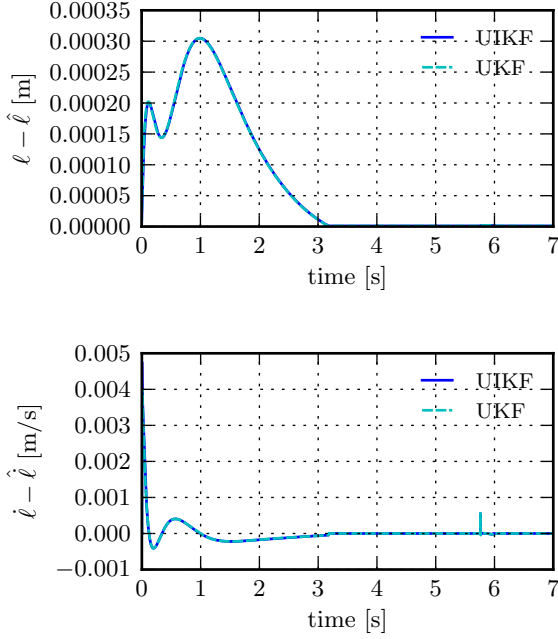


Figure 6: Error of the position and velocity estimations

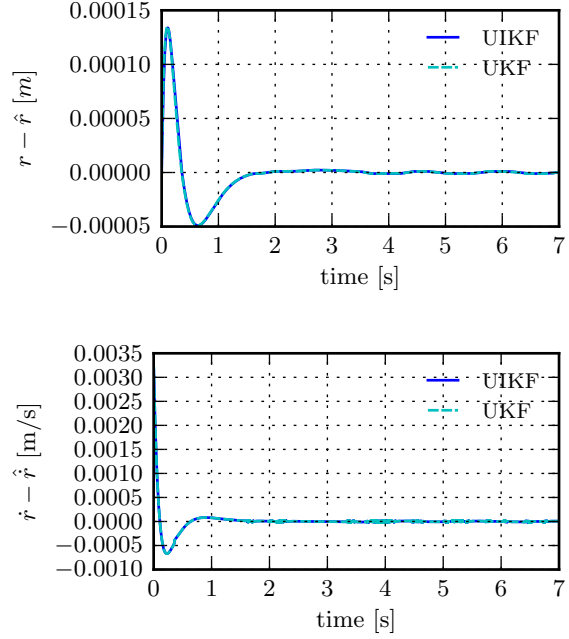


Figure 7: Error of the rope length and hoisting velocity estimations

much less than the actuating signals. The large offset in Fig.4 is a consequence of the stiction, the cart will not move until u_F becomes greater than a certain value (in our case about 28 N). When the cart finally stops moving, the fluctuation of u_F tries to counter the load sway, during which the measured states do not change. This is the reason why the estimators find the input to be zero.

Fig.5 shows the transient of the states in a closed-loop. Results show that the controller can bring the system into the desired state, but friction prevents it from stopping the low amplitude swinging of the load, because it makes quick, short motions impossible. Error estimates are illustrated by Figs. 6 and 7. In all cases, the error becomes zero when the crane reaches the desired state.

This is not true for the angle and its derivative in Fig.8. The error decreases at the end of the state transient, but does not become zero. When the cart stops and the load swings, the measurements are all constant thus they carry no information regarding θ and $\dot{\theta}$. In these situations the cart and winch are usually also motionless due to friction. Consequently, the estimation error of these quantities never becomes zero.

It is possible to decrease the estimation error using two laser slot sensors. With the help of such devices, θ can be measured accurately in two positions and through the application of proper sensor fusion techniques the estimation of the angle can become more precise in between the chosen positions as well.

In Fig.9 the estimation error of θ and $\dot{\theta}$ is illustrated using CKF. The filter was designed for the dynamics given by Eq.(7) except that it does not consider the inputs unknown. The results show that the error is substantially higher than in the case of the UIKF or UKF.

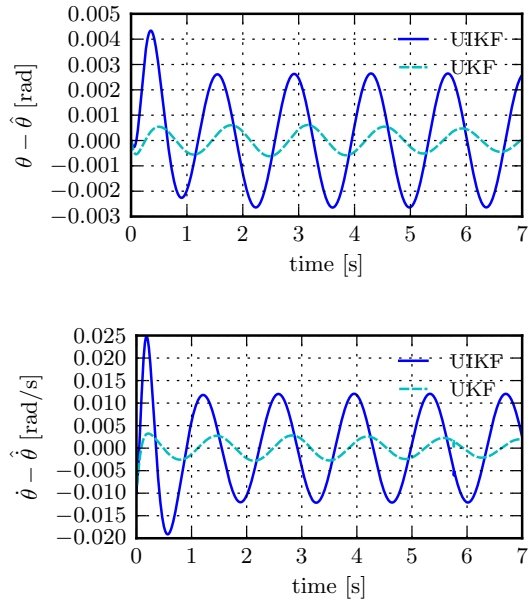


Figure 8: Error of the angle and angular velocity estimations

Fig.8 shows the estimation error of the UKF to be less. We applied this estimator in a closed-loop scenario identical to the one presented in Fig.3, but instead of $x[k]$ the $\hat{x}[k]$ of the UKF was used in the feedback loop. The state evolution of the crane in this simulation is illustrated in Fig.10. The system's behaviour is only slightly different from the case when the actual states were used in the feedback control in Fig.5.

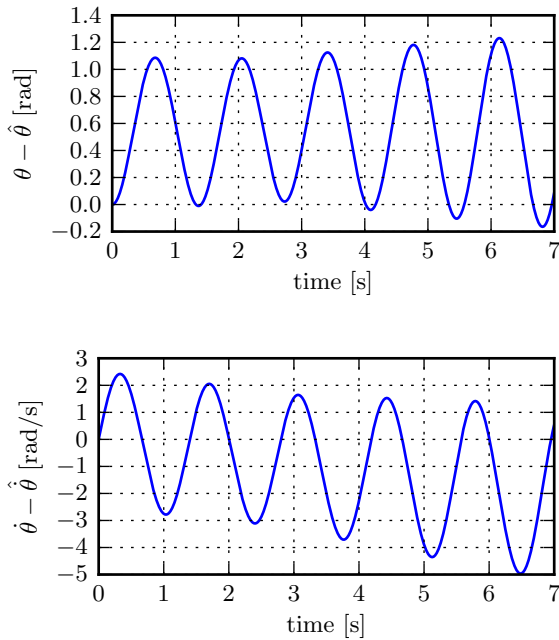


Figure 9: Error of the angle and angular velocity estimations using CKF

Conclusion

It was shown that in most mechanical systems the disturbing effect of friction can be reduced to the actuating signals. Based on this statement, two estimation methods were provided for the computation of the unmeasured states. One of these techniques considers the inputs completely unknown and uses UIKF for the estimation. The other algorithm treats the inputs as distorted by an additive disturbance, and applies UKF with a load predictor extension. Simulation results in a closed-loop controlled scenario were provided to prove the applicability of the concepts. It was also pointed out, that the precision of the estimators could be improved using laser slot sensors. This will be the subject of a forthcoming paper.

REFERENCES

- [1] HYLA P.: The crane control systems: A survey, Proc. 17th Int. Conf. Methods and Models in Automation and Robotics (MMAR), 2012, 505–509
- [2] SCHINDELE D., MENN I., ASCHEMANN H.: Non-linear optimal control of an overhead travelling crane, Proc. 18th IEEE Int. Conf. Control Applications, 2009, 1045–1050
- [3] BOUSTANY F., D'ANDREA NOVEL B.: Adaptive control of an overhead crane using dynamic feedback linearization and estimation design, Proc. IEEE Int. Con. Robotics and Automation, 1992, 1963–1968

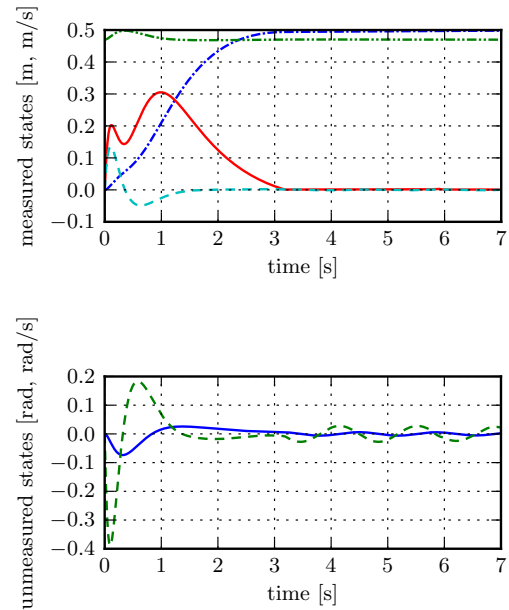


Figure 10: State evolution of the controlled crane using the UKF's estimated states as feedback

- [4] NEUPERT J., HILDEBRANDT A., SAWODNY O., SCHNEIDER K.: Trajectory tracking for boom cranes using a flatness based approach, Proc. Int. Joint Conf. SICE-ICASE, 2006, 1812–1816
- [5] RÓZSA T., KISS B.: Tracking control for tow-dimensional overhead crane, Proc. 8th Int. Conf. Informatics in Control, Automation, and Robotics, ICINCO, 2011, 1, 427–432
- [6] KISS B., LEVINE J., MULLHAUPT P.: A simple output feedback PD controller for nonlinear cranes, Proc. 39th IEEE Conference on Decision and Control, 2000, 5, 5097–5101
- [7] KISS B., LÉVINE J., MÜLLHAUPT P.: Modelling, flatness and simulation of a class of cranes, Electrical Engineering, 1999, 43, 215–225
- [8] LANTOS B.: Theory and design of control systems I., Akadémia Kiadó, 2001 (in Hungarian)
- [9] DAROUACH M., ZASADZINSKI M., ONANA A.B., NOWAKOWSKI S.: Kalman filtering with unknown inputs via optimal state estimation of singular systems, Int. J. Sys. Sci., 1995, 26(10), 2015–2028
- [10] HAYKIN S.S.: Kalman filtering and neural networks, John Wiley & Sons, Inc., 2001
- [11] ARMSTRONG-HÉLOUVRY B., DUPONT P., DE WIT C.C.: A survey of models, analysis tools and compensation methods for the control of machines with friction, Automatica, 1994, 30, 1083–1138
- [12] KALMAN R.E.: A new approach to linear filtering and prediction problems, Journal of basic Engineering, 1960, 82, 35–45